



REGULAR ARTICLE

Design, Fabrication and Measurements of an X-Band Cross-Patch Antenna with Metasurface for Advanced LEO CubeSat Missions

B. Benhmimou^{1,*} ✉, F. Omari¹, N. Gupta², K. El Khadiri³, A. Kogut⁴, R.A. Laamara¹, I. Kuzmichev⁴,
M. El Bakkali^{1,3,†}

¹ LPHE-MS, Faculty of Sciences, University Mohammed V in Rabat (UM5), Rabat, Morocco

² ECE Department, Lyallpur Khalsa College Technical Campus, Jalandhar, Punjab, India

³ Department of Physics, Faculty of Sciences El Jadida, University Chouaib Doukkali of El Jadida, Morocco

⁴ O.Ya. Usikov Institute for Radiophysics and Electronics of NAS of Ukraine, Kharkov 61085, Ukraine

(Received 25 March 2025; revised manuscript received 20 June 2025; published online 27 June 2025)

In this research, we build, miniaturize, and optimize a smart metasurface antenna to meet the requirements of the smallest cube satellite unit with almost negligible air drag altitude. One of the main objectives of this study is to extend the AeroCube lifetime by adopting far orbits and obtaining significant HPBW angles in order to increase the data reception period throughout the day while using a very efficient energy system. To accomplish all of this, a new antenna shape was adopted, consisting of planar dipole antennas perpendicular to each other, to minimize size to the greatest extent possible while maintaining good operating characteristics in accordance with all previous objectives, without the need for any antenna deployment process after the satellite reaches orbit. Furthermore, a completely new unit cell shape was adopted and optimized to create the metasurface layer, allowing for further enhancement of the final X-band antenna characteristics and, as a result, the overall efficiency of the completed cube satellite. The designed metasurfaced antenna was well manufactured and validated in the anechoic chamber and using vector network analyzer, yielding satisfactory measured results in X-band for CubeSat communication. It is lightweight and exhibit unidirectional radiation pattern with wide 3 dBi gain bandwidth (3 dBi GBW of about 1.0 GHz) and high gain of about 10.0 dBi at 8.4 GHz. The overall results with occupied size and volume are satisfactory for unlimited lifetime CubeSat missions at X-band using all CubeSat structures.

Keywords: 1U CubeSat, Antenna measurements, Cross-patch antennas, CubeSat lifetime, MTM, Peak gain

DOI: [10.21272/jnep.17\(3\).03007](https://doi.org/10.21272/jnep.17(3).03007)

PACS number: 84.40.Ba

1. INTRODUCTION

In the second decade of the twentieth century, cube satellite technology witnessed an amazing development to the point that it became widespread in most countries on all continents. Today, we are talking about thousands of CubeSat missions operating in different orbits around the Earth for several purposes. These include weather monitoring, studying climate change such as monitoring the melting of ice at the poles, studying river levels during the year, regulating ship traffic in ports, regulating air traffic at airports, acting as an intermediary between integrated missions to increase the rate of data flow to the Earth, etc., and commercial and military purposes as well [1]. In addition, the availability and multiplicity of means that can deliver these small satellites to their orbits at a low cost has led to the transition to talking about daily launch rates with very important proportions. For example, Falcon, Vega, PSLV

and similar rockets successfully launch several cube satellite missions to different orbits on a regular basis, regardless of whether they are governmental or private [2]. This tremendous technological boom has led to amazing progress in the engineering of all the devices of a specific cube satellite mission according to the coordinates and objectives of the mission. For example, there are several international commercial companies that provide all the parts of a cube satellite and the rest are assembled correctly in just a few days or a few weeks. For example, GOMspace and Kongsberg NanoAvionics companies supply ready-made designs for most devices and pieces, which may be assembled to create any cubic satellite configuration [3, 4].

In general, the smallest cubic satellite has mass of about 1.33 kg and delivers a few watts to the majority of its electronics, making designing and manufacturing these devices rather than acquiring them a goldmine for space technology researchers [5]. In this context, one of

* Correspondence e-mail: boutaina.benhmimou@um5.ac.ma

† mohamed.elbakkali1617@gmail.com



the most significant devices is the design and production of cubic satellite antennas, which are responsible for exchanging communications with base stations and therefore achieving the goals of the lunar mission in general [6]. It should be emphasized that many of the successfully launched cubic satellite missions were carried out in Low-Earth orbit, where air exerts a considerable drag effect on composite satellite interfaces, causing damage to the devices over time [7]. Thus, a low drag coefficient indicates less aquatic mechanics and aerodynamic resistance within the CubeSat box, extending the satellite's life. As a result, each satellite mission's top objective is to reduce the influence of air resistance on the satellite while it is in orbit. Add to this the necessity to establish radio links between the satellite in orbit and the ground operators so that data and commands may be exchanged as long as feasible during the day, regardless of weather conditions. Data is delivered to ground operators for a few minutes each day. Thus, the elements influencing the quality of connection between the satellite and the Earth's operators are highly sensitive to the overall performance of the consultancy within the targeted precipitation of consumers [8]. The total loss during any continuous operation includes any retention of signal quality from the satellite to the ground station [9, 11]. The distance of the bilateral radio communication pattern is determined by the satellite's height angle and the angle between its orbit point and ground stations, which, along with current satellites' tiny size, restricts the feasibility of a secondary deployment of the antenna in orbit [10] [12, 13]. Bypassing the secondary deployment of satellite antennas is one of the mission's most essential technical objectives for aerospace engineers [14]. By maintaining radio communication between the satellite, which orbits the Earth multiple times a day, and the ground stations, which are stationary and have little ability to alter the communication angle based on the satellite's point of presence during its movement, the best service is provided to operators on Earth and, consequently, customers. These grandparents will live forever thanks to the nearly complete lack of air resistance when circling and the high-energy solar radiation that quickly charges satellite batteries. To be more precise and comprehensive in this context, this article focused on the utilization of the smallest cubic satellites, which are typically utilized in low Earth orbits for only a few years. In this regards, this article aims to construct a lightweight and extremely effective cross-patch antenna with metasurface (MTM / MTS) for very advanced Earth orbits using the Smallest configurations, 1U AeroCubes.

This research paper aims to construct a small and lightweight antenna configuration on 1U CubeSats by pursuing three primary objectives. In the first, HFSS's FEM approach and QNM package are used to design, downsize, and optimize a planar crossed dipole antenna that can occupy an area less than 8% of a 1U CubeSat face. Other frees up more space will be used by other components like solar arrays, radars, surveillance

systems, and so on. In order to raise the appropriate orbit radius and, consequently, the CubeSat lifetime itself, the second objective is to use metasurface (MTM / MTS) to improve antenna performance at the same operating frequency while concurrently increasing the daily sent data throughput. More precisely, we seek to reduce interference with other components inside the 1U CubeSat box and then optimizing antenna peak gains, 3dBi gain bandwidths, and beamwidth angles. The third purpose is to evaluate the fabricated cross-patch antenna alone and the whole MTM antenna prototypes by measuring their features and comparing them to the simulation results to see how well they performs for 1U CubeSat missions. As a result, the goal of this contribution is to optimize new cross-patch antenna and tiny metasurface configurations in order to build high performance small-sized antenna systems suitable for use on 1U CubeSats with an area of less than 8%. This will serve to both increase gain and reduce size at 8.4 GHz. Specifically, the authors combine cross-patches and a novel unit cell layout to create a new MTM antenna that can satisfy all of these criteria while also being low cost, lightweight, and low volume. Additionally, the high stiffness of the developed CubeSat architecture (i.e., Full system), the fulfillment of requirements proposed by 1U CubeSat deployed systems, and the ability to operate in space at extremely high speeds all contribute to its utility for advanced LEO AeroCube missions.

This study is arranged as follows: Section 2 describes the geometrical specifics of the proposed MTM antenna design, fabrication, and measurement block. This section illustrates and explains the geometrical characteristics and measuring procedure of the suggested antenna approaches. In Section 3, the recommended techniques are discussed and analyzed in depth using parametric analysis. It also demonstrates the efficacy and benefits of the proposed MTM antenna for CubeSats in X-band. Section 3 provides a comprehensive comparison of our proposed antenna design to previous efforts on CubeSat antennas that employ metasurface and other techniques to X-band patch antennas. Finally, section 4 summarizes our contributions to this study endeavor.

2. ANTENNA DESIGN, FABRICATION AND MEASUREMENT BLOCK

This paper proposes to design an X-band (8.4 GHz) cross-patch antenna developed and optimized using ANSYS HFSS for optimal operation on a 1U CubeSat [15] in order to combine the characteristics of the smallest size and the highest performance, making it suitable for all AeroCube standards. The cross-patch elements are printed on the top face of the low cost Rogers RT 5880 dielectric ($\epsilon_r = 2.1$, $\tan\delta = 0.001$ and $h = 1.5$ mm) which considered as substrate material because of its wide availability in the market and high reliability characteristics for AeroCube applications [16] [17]. Fig. 1 depicts the design evolution of proposed cross-patch antenna system and shows that it is feed

using a 50-Ω CPW feed-line having dimensions of $5 \times 3.5 \text{ mm}^2$. All antenna dimensions are estimated using the HFSS FEM method and optimized using a special QNM approach. Its purpose is to construct a tiny and lightweight MTM antenna suited for all CubeSat designs, with a gain more than 10.0 dBi and a broad - 10dB BW at X-band (8.4 GHz). The QNM approach is used to compute the antenna dimensions at 8.4 GHz by altering their initialization values over 1000 iterations in order to achieve the desired return loss and peak gain at 8.4 GHz while maintaining size and volume appropriateness for all CubeSat designs, including the 1U form. To solve the challenges associated with using dielectric substrates in the high frequency region, we suggest an MTS structure, as seen in Fig 2(a). This MTS architecture is made up of an array of square unit cells optimized using the approach shown in Fig. 2(b). The resultant structure was effectively employed to create a small-sized MTS antenna, see Fig. 2(c). The optimized design covers just 6.84 % of a 1U CubeSat's top face ($10 \times 10 \text{ cm}^2$) and appears to be exceptionally rigid, lightweight, and compact, making it suitable for usage with any CubeSat architecture.

The antenna fabrication procedure was then carried out individually for both the cross-patch antenna and the whole MTM antenna system to confirm the aforementioned simulation results, as well as to evaluate the physical performance and efficacy of suggested antenna approaches. The vector network analyzer's 50Ω port was used to test the $|S_{11}|$, VSWR, gain parameters as a function of frequency, and the 2D radiation pattern characteristics for the constructed cross-patch antenna prototype by itself and the prototype of the whole MTM antenna. The fabrication and testing procedure are shown in Figs. 3 and 4, where the antenna is connected coaxially to vector network analyzer (VNA) port.

The most crucial phases of a CubeSat-earth station link are depicted in Fig. 5 below. It demonstrates how each transmission link's characteristics, the data rate of a CubeSat-Earth station transmission, and ultimately the mission's lifetime is determined by the transmitting antenna's power and gain in parallel with the receiving antenna's power and receive gain.

Furthermore, it is demonstrated that the entire MTM antenna takes up a small area on the smallest CubeSat standard (1U), while solar panels use nearly all of the available space to generate energy, which is extremely constrained on CubeSats. Additionally, it is demonstrated how to calculate the limits of physical area and volume that any CubeSat antenna can occupy at the same time, along with the performance requirements based on the desired wave length, CubeSat configuration, frequency, and orbit radius, and thus the CubeSat lifetime itself.

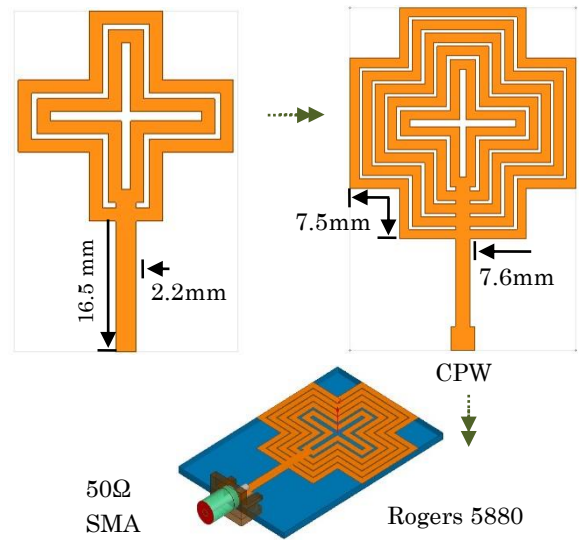


Fig. 1 – Configuration, evolution and Dimensions of proposed cross-patch antenna

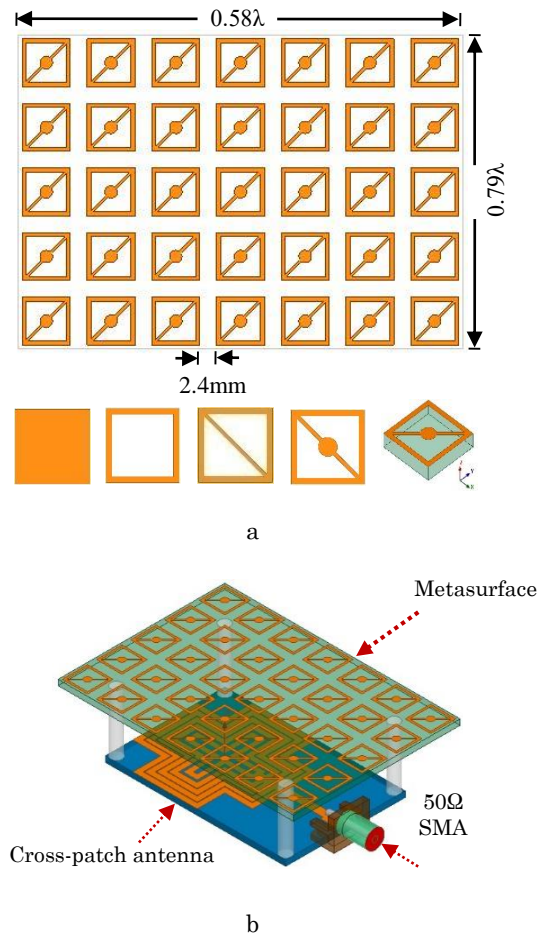


Fig. 2 – Configuration of developed metasurface antenna system, (a): Unit cell configuration and proposed metasurface, (b): 3D Layout of proposed MTM antenna

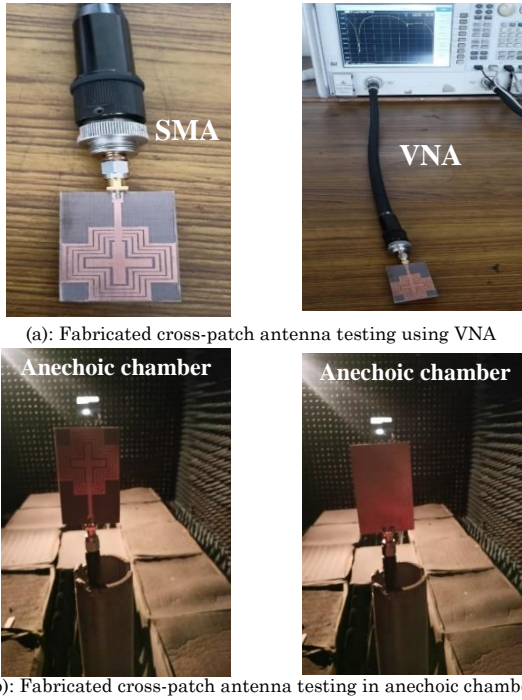


Fig. 3 – Prototype of the fabricated cross-patch antenna and its measurement blocks

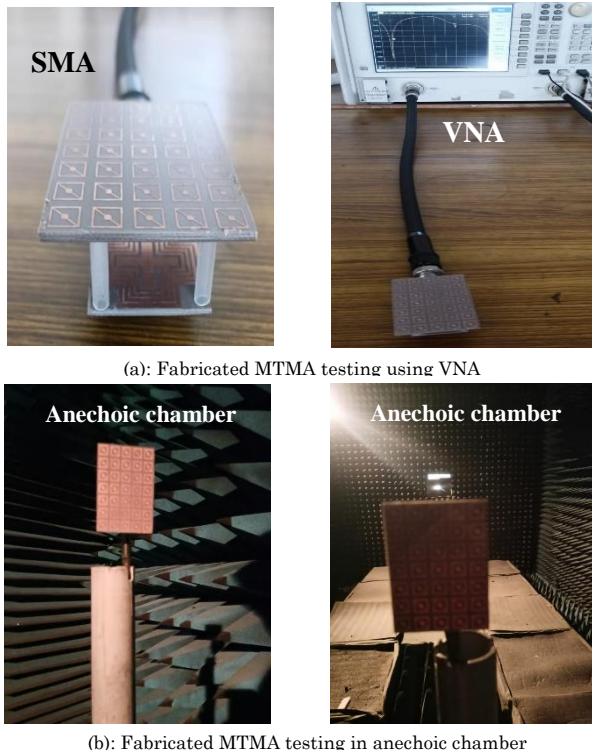


Fig. 4 – Prototype of the fabricated metasurface antenna and measurement blocks

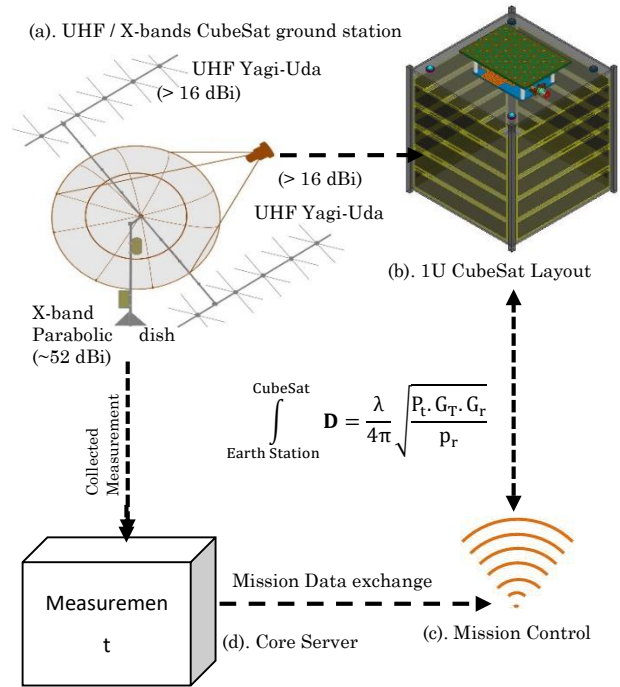


Fig. 5 – Protocol of proposed 1U CubeSat antenna - UHF/X-band Ground Station Links

Fig. 6 below illustrates how air density and, consequently, its resistance on the satellite interface affects the lifetime of the CubeSat mission. For example, the pressure on the satellite's interface increases sharply the closer we get to the Earth's surface, to the point that the satellite's life span does not exceed a few months to a year or two at most. This is due to the fact that the air density is higher near the Earth's surface than at altitudes exceeding 1000 kilometers. For example, Fig. 6 shows the big difference between the life spans of satellite missions at altitudes of 450, 500, and 600 kilometers, where the largest life spans are at 600 kilometers, regardless of the air drag values depending on the size of the satellite and thus the area of its interface. In addition, it appears that the life span of a cube satellite mission becomes indefinite, i.e. it is not affected by the effects of air in the event that it orbits the Earth from altitudes exceeding a thousand kilometers. Accordingly, the superiority of cube satellite missions over others is due to the type of missions they perform and their resistance to air effects by targeting high altitudes exceeding a thousand kilometers or reducing the area of the cube satellite's interface and thus overcoming the effects of air drag.

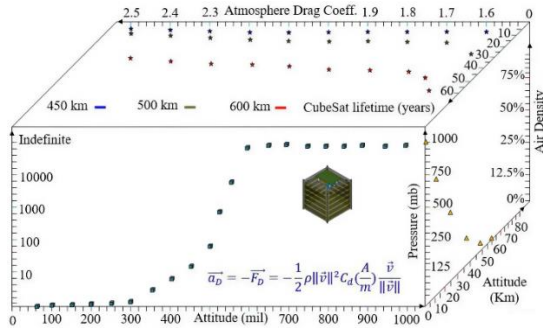


Fig. 6 – 1U and 3U CubeSat lifetime (years), Pressure, Air density, and Atmosphere drag vs. attitude (Km or Mile)

The aforementioned demonstrates that the process of creating this X-band metasurface-based antenna that will be utilized in 1U CubeSats offers numerous opportunities for research and development in three distinct directions: lowering the electrical energy required for the antenna's design and development in order to supply it to the other devices or lessening the strain on the satellite's electrical energy production system. In order to accomplish the first aim, the second goal is to minimize the size and area while avoiding, as far as possible, a secondary deployment procedure that is unique to the device. The third purpose is to maximize the antenna's attributes in order to increase the efficiency of completed missions and target very high orbits, such as those with very extended life spans, as previously noted.

3. RESULTS, DISCUSSION, AND SUMMARY OF ACHIEVED RESULTS

As previously stated, this antenna approach is built around the unique antenna parameters that effect a CubeSat mission while still meeting consumer requirements. The analysis of all simulated and measured results will now be done in terms of a CubeSat mission under development by engineers and consumers inside the laboratory, taking into account the entire CubeSat lifetime from design to the end of its lifetime in orbit around Earth. To further demonstrate how effective this antenna strategy is for CubeSat standards, the design evolution, result improvement, and measurement setup will be presented in a similar manner. Fig. 7 depicts the E-field, H-field, and antenna gain at 8.4 GHz for a cross-patch antenna constructed using two elements. It demonstrates that this design radiates unidirectionally and achieves a peak gain of 5.5 dBi at 8.4 GHz, making it suitable for usage on CubeSats for inter-CubeSat and CubeSat swarm communication.

Based on that, this design is enhanced by employing five components to create the source antenna, which provides two effective bands at the X-band, as seen in Fig. 8 showing the results of measured and simulated reflection coefficients. The measurement results indicate that the lowest measurements of $|S_{11}|$ are -26.5 and -30 dB at 8.38 and 8.81 GHz, respectively. Furthermore, as both findings exhibit measured

impedance bandwidths of 160 and 780 MHz and simulated impedance bandwidths of 170 and 410 MHz for X-band CubeSat communication, the measured and simulated results are in good agreement. Thus, both simulation and measurement demonstrate the dual-band nature of the improved cross-patch antenna design, allowing earth stations and other transmitting spacecrafts to connect with the designed CubeSat antenna using two effective bands independently. It enhances the sent data rate because the CubeSat has just a few minutes per day to connect with Earth as normal.

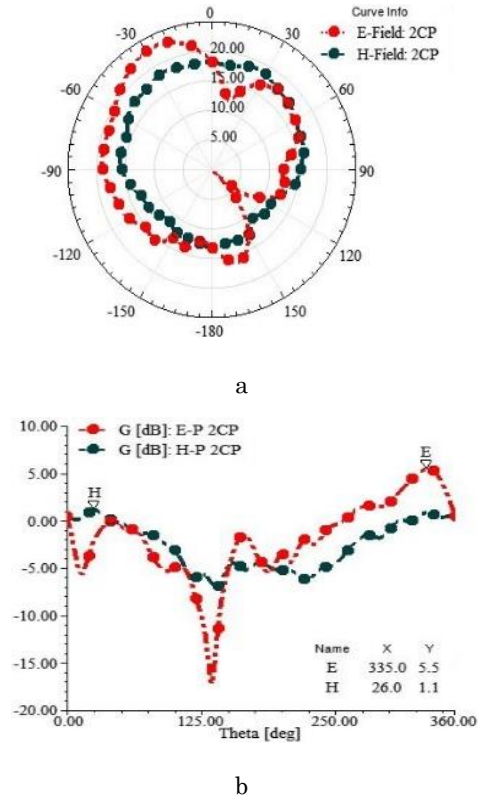


Fig. 7 – E- and H-fields and Antenna Gain at 8.4 GHz of two elements based cross-patch antenna, (a) 2D radiation pattern of the two crossed-patch antenna design at 8.4 GHz, (b) 2D gain plot of the two crossed-patch antenna design at 8.4 GHz

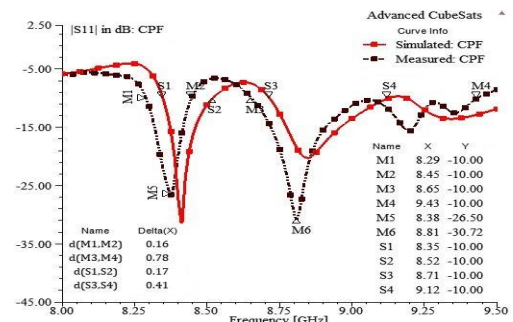


Fig. 8 – Measured and Simulated $|S_{11}|$ of proposed Cross-Patch antenna

To be more beneficial, because the bilateral transmission between a CubeSat and Earth stations takes just a few minutes each day, it is preferable to maximize the acquired performance in accordance with the geometrical, mechanical, and electrical requirements of every CubeSat mission. In this sense, this antenna approach creates an optimal metasurface of 5×7 unit cells with the current distribution shown in Fig. 9(a). It exhibits practically uniform current distribution as a result of the extremely powerful optimization applied to the novel form of metasurface unit cell with reflection phase investigated and illustrated in Fig. 9(b). The suggested metasurface exhibits a broadband response, with the zero-degree reflection phase at 8.4 GHz and a reflection phase bandwidth ($\pm 10^\circ$) ranging from 8.0 GHz to 8.8 GHz. The effectiveness of these results and the optimal choice of unit cell to build the generated metasurface are demonstrated by simulated results and measured findings of bandwidth enhancement [18], as shown in Fig. 10.

When compared to the cross-patch antenna alone, the optimized metasurface antenna's measured and computed reflection coefficient findings, displayed in Fig. 10, demonstrate high agreement and bandwidth improvement. The calculated $|S_{11}|$ parameter is almost -20 dB at 8.4 GHz, yet the measurement indicates an extremely low reflection coefficient of -31.3 dB at the same frequency. Furthermore, the computed and measured impedance bandwidths are much improved. The first simulated -10 dB BW is extended from 170 MHz (cross-patch antenna alone) to 210 MHz (metasurface antenna), while the second impedance bandwidth is increased from 410 MHz (cross-patch antenna alone) to 690 MHz (metasurface antenna). Additionally, the experiment reveals an infinite impedance bandwidth spanning from 8.21 GHz to 9.5 GHz.

On the other hand, the measurements of the $|S_{11}|$ coefficient match well with the calculated values around an operating frequency of 8.4 GHz. These achievements are well proven by the findings of VSWR coefficient and antenna gain, which are shown in Fig. 11. The metasurfaced antenna provides two VSWR bandwidths, 8.36 to 8.58 GHz and 8.75 to 9.49 GHz, respectively.

Added to that, when compared to the cross-patch antenna alone, the generated metasurface provides significant VSWR increase, see Fig. 11(a). Fig. 11(b) shows that the optimized metasurface increases antenna gain by over 16% (more than 1.5 dBi) at the same operating frequency while occupying the same area on the CubeSat box. Power consumption remains low as the entire antenna system is excited using a 50Ω SMA connector. At the same operating frequency, the cross-patch design alone yields peak gain of around 8 dBi, whereas the metasurfaced antenna provides peak gain of about 10.0 dBi. As a result, both designs are optimal for usage on compact CubeSat configurations with advanced LEO AeroCube missions. Moreover, the simulated and actual 2D radiation patterns correlate well, as seen in Fig. 12.

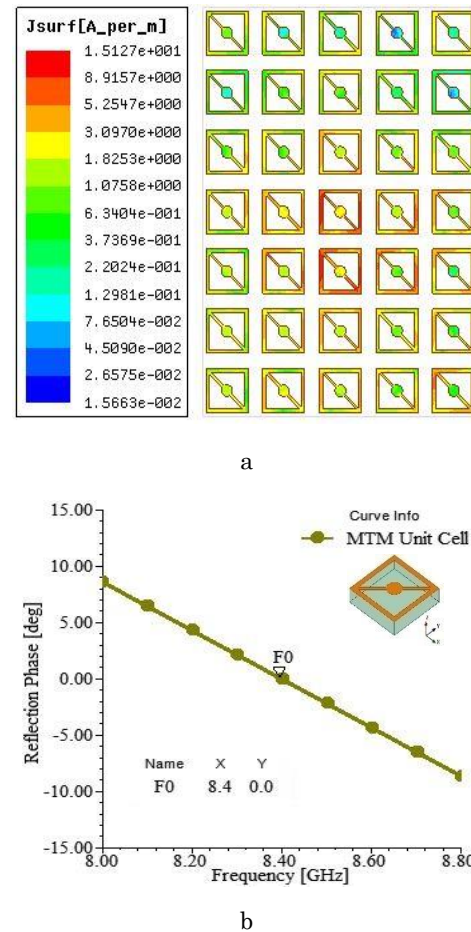


Fig. 9 – Current distribution of Constructed MTS and reflection phase of unit cell metasurface, (a) Current distribution of Constructed MTM at 8.4 GHz, (b) Reflection Phase on unit cell

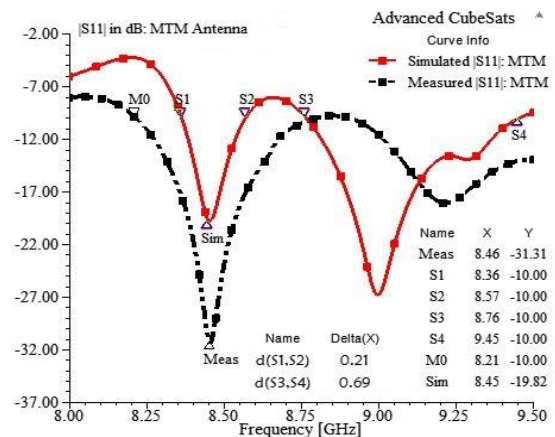


Fig. 10 – Measured and Simulated $|S_{11}|$ parameter of proposed MTM antenna

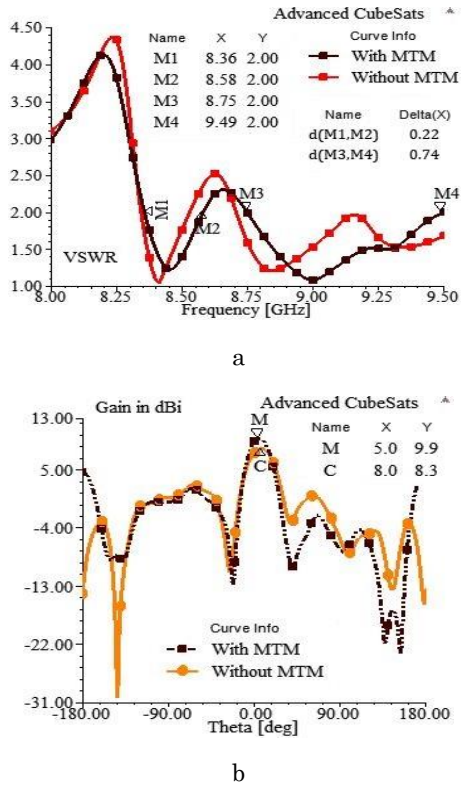


Fig. 11 – VSWR and gain plots of proposed Cross-Patch antenna with and without MTM, (a) VSWR coefficient vs Frequency, (b) Gain plots at 8.4 GHz

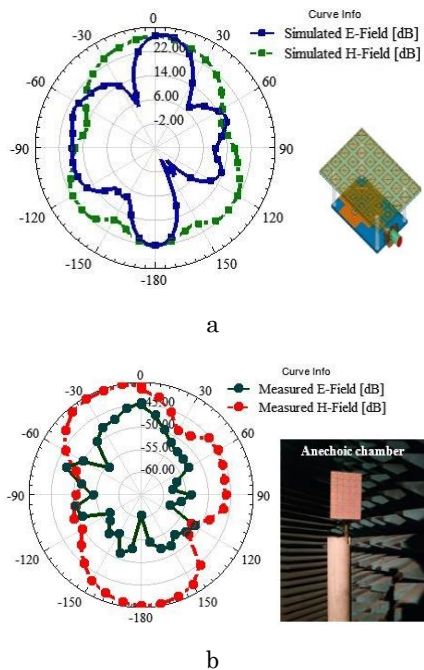


Fig. 12 – Measured and Simulated 2D radiation patterns of designed and fabricated MTM antennas at 8.4 GHz, (a) Simulated 2D RP of simulated MTM antenna, (b) Measured 2D RP of fabricated MTM antenna

Both simulated and measured radiation patterns have large beamwidth angles and are appropriate for CubeSat communication due to the majority of electro-magnetic energy is emitted beyond the CubeSat shell. Furthermore, the experimental measurement of the antenna gain parameter shown in Fig. 13 demonstrates that the manufactured metasurface antenna provides gain greater than 8.0 dBi throughout a wide 3 dBi gain bandwidth extending from 8.0 to 8.9 GHz. These two points are one of the most significant achievements of this antenna design since they enable deep link communication between the proposed CubeSat configuration and earth stations or other spacecraft circling the planet Earth. The broad beamwidth angle conserves transmission for various CubeSat elevation angles, and the high gains ensure that data and orders are properly received. Tables 1 and 2 numerically describe all of these achievements, as well as the metasurfaced antenna's geometrical and mechanical attributes.

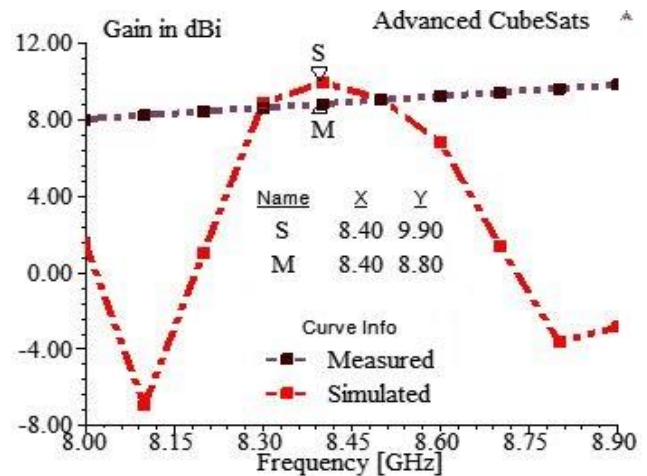


Fig. 13 – Measured and Simulated Gain of constructed MTM antenna

Table 1 – Physical and electrical characteristics of the fabricated cross-patch and metasurfaced antennas at X-band (8.4 GHz)

Characteristics	Cross-Patch antenna	Metasurface Antenna
Dielectric constant (Rogers 5880)	2.1	2.1
Dielectric thickness (Rogers 5880)	1.5 mm	1.5 mm
Physical size	32.4 × 48.9 mm ²	0.58 λ ₀ × 0.79 λ ₀
Operating frequency	8.4 GHz	8.40GHz
Return Loss	~ 26.5	~ 31.0
VSWR	Close to one	Close to one
Beamwidth angle	×	Very wide
Radiation Pattern	Unidirectional	Unidirectional
Back lobes	Minimum	minimum
Gain	8.3 dBi	~ 10.0 dBi

Table 2 – Suitability and Geometrical / mechanical Analysis according to all CubeSat standards: 0.5 U, 1U, 2U, 3U and 6U

Characteristics	MTM antenna
Surface / 0.5U CubeSat's top face (10 × 5 cm ²)	57 %
Volume / 0.5U CubeSat's volume	8.65 ‰
Surface / 1U CubeSat's top face (10 × 10 cm ²)	28.8 %
Volume / 1U CubeSat's volume	4.32 ‰
Surface / 2U CubeSat's top face (10 × 20 cm ²)	14.4 %
Volume / 2U CubeSat's volume	2.16 ‰
Surface / 3U CubeSat's top face (10 × 30 cm ²)	9.6 %
Volume / 3U CubeSat's volume	1.44 ‰
Surface / 6U CubeSat's top face (20 × 30 cm ²)	4.8 %
Volume / 6U CubeSat's volume	0.72 ‰
Power consumption	Very low
Radiation	Directional antenna
Beamwidth Angle	Very wide
Interferences with CubeSat subsystems	Minimum
Power dissipation	Negligible
Gain	~ 10.0 dBi
Cost	Very low (< 100 \$)
Mass	Lightweight
Suitability for All CubeSat Configurations	Very suitable

This means that the developed 1U configuration can be used for hundreds of years after the satellite launch due to the absence of atmospheric drag at high altitudes, small sectorial area, low mass and high antenna gain of proposed 1U CubeSat configuration. In addition to that, the other CubeSat configuration can be targeted as high altitude satellite missions using the constructed metasurface antenna system since their masses and sectorial areas are close to each other. From another

hand, the achieved wide band, wide HPBW and wide 3 dBi gain bandwidth make the whole configuration suitable to communicate simultaneously with several earth stations located in different places.

4. DETAILED COMPARISONS WITH LITERATURE WORKS

As it is mentioned before, the X-band is extensively studied because of its potential to design high-performing medium- and small-sized planar antennas. In Tables 3 and 4, the constructed metasurface antenna system is compared with 18 similar X-band antenna designs that can be used for CubeSats in terms of geometrical parameters or electrical properties. Not that the suitability for a CubeSat mission is studied in terms of geometrical, mechanical and electrical characteristics of each antenna design. An antenna system can be used for a CubeSat configuration if it satisfies all geometrical, mechanical and electrical requirements of the CubeSat mission. Hence, the goal of this comparison is to balance the trade-off between improving the antenna performances for direct-to-Earth communications and maintaining geometrical suitability for all CubeSat configurations, including 0.5U and 1U structures. This results in a metasurface unit cell that is smaller than 1 cm by 1 cm in compact area, making the whole metasurface-based antenna adaptable to any CubeSat layout. Tables 3 and 4 show that both the cross-patch antenna and the developed metasurface antenna are compared to 16 X-band AMC, metamaterial, and metasurface-based antennas with physical sizes suitable for 1U CubeSats, with the majority geometrically and mechanically suitable for 0.5U structures. They are mechanically and geometrically perfect for use on CubeSats since they are lightweight, require no deployment equipment, and consume very little power. These X-band metasurface antenna designs are thoroughly examined in terms of physical dimensions, operating frequency, materials, polarization, forms of realized radiation patterns, and the amount of created interference.

Table 3 – Geometrical comparison with various metasurface and AMC-Based Antenna Designs for CubeSats at X-band

References	Total antenna size	Operating Freq. [GHz]	Materials
[19]	5×26×0.5mm ³	6.9 - 8.8	Jeans textile, Copper
[20]	40×30×0.8mm ³	9.70	metallic ring; Rogers 4003C
[21]	25.2×23.7×10mm ³	8.30	RT/duroid 5880 (0.5 mm-thick), Copper
[22]	55×55×17.67 mm ³	10.00	FR-4; copper film
[23]	30×22×1.6mm ³	10.10	FR4 (0.6 mm-thick), Copper
[24]	12×12×3.58mm ³	8.95-10.68	Rogers RT5880; Rogers RO4030; Copper
[25]	140×140mm ²	8.82, 9, 9.25, 9.43, and 10.1	FR4; copper
[26]	28×28mm ²	10.44; 10.77; 10.94	FR4; Teflon; Copper
[27]	~74×74mm ²	9.5-10.2 (LP) and C10.2-10.8 (CP)	Rogers 5880; Plastic pole
[28]	~24×24×2.004 mm ³	10.0	F4B; Rogers 4350B
[29]	50×50 mm ²	7.80; 8.10	Kapton layer; FR4
[30]	~31.2×31.2×4.5mm ³	7.47-11.65	Rogers 4350B; Rogers RT5880 ; Copper
[31]	62×62× 22.2mm ³	8.28 -8.88	RO3003, Copper
[32]	~81.75×81.75×14.3mm ³	10.90; 22.50	Copper; PCMs; vanadium dioxide Graphene
[33]	60×60×7.92mm ³	7.14 - 8.45 and 7.10 - 8.70	Rogers 5880, Copper
[34]	29×29×2 mm ³	8.40	Rogers RO 4003, copper
Cross-patch antenna	32.4×48.9×1.5	8.40	Rogers 5880; copper
Metasurfaced antenna	32.4×48.9×3	8.40	Rogers 5880; copper

Table 4 – Electrical comparison with various metasurface and AMC-Based Antenna Designs for CubeSats at X-band

References	Operating Freq. [GHz]	Gain [dBi]	Bandwidths [GHz]	Polarization	Radiation Pattern	Interferences
[19]	6.9 - 8.8	6.17	6.9-8.8	Circular	semi-omnidirectional	Medium
[20]	9.70	8.43	~1.60	Linear	Unidirectional	Low
[21]	8.30	1.70	~8.0-10.0	Linear	bidirectional	Minimum.
[22]	10.00	9.45	9.42 - 10.62	linear	unidirectional	Reduced
[23]	10.10	7.20	8.50 - 11.30	circular	unidirectional	Low
[24]	8.95-10.68	5.85	IBW: 8.95-10.68 ARBW: 10.62-11.87	Circular	Unidirectional	Minimum
[25]	8.82, 9, 9.25, 9.43, and 10.1	Not assigned	8.5 - 10.5	Linear	Unidirectional	negligible
[26]	10.44; 10.77; 10.94	7.57	10.14 - 10.94	Linear	Unidirectional	Medium
[27]	LP: 9.5-10.2 CP: 10.2-10.8	10.00	8.0 - 12.0	Circular	unidirectional	Low
[28]	10.0	8.60	8.41 - 11.67	RHCP	Unidirectional	Very low
[29]	7.80; 8.10	8.60	7.25 - 8.40	circular	Bidirectional	High
[30]	7.47-11.65	H: 6.58 - 7.68 V: 5.85 - 7.28	43.72%: Port H 38.65%: Port V	Linear	Quasi-omnidirectional	Low
[31]	8.28-8.88	7.0	-10dB BW : 8.0-9.5 3dB ARBW: ~8.3-8.8	LHCP	Unidirectional	Low
[32]	10.90	8.40	3dB ARBW: 10-12.54	LHCP RHCP	Unidirectional	Low
[33]	7.14 - 8.45 7.10 - 8.70	7.6±1.50 7.4±1.80	66.7% (3.1–6.20) 20.3% (7.1–8.70)	circular	Unidirectional	Low
[34]	8.40	5.80	8.28-8.59	Linear	Unidirectional	Low
Cross-patch antenna	8.40	8.30	IBW: 0.16; 0.78	Linear	Unidirectional	Low
Metasurfaced antenna	8.40	~10.0	3dBi GBW > 1.0 IBW > 1.31	Linear	Unidirectional	Low

Table 5 – Comparison with some similar works which use Patch antennas at X-band

Reference	F ₀ [GHz]	Volume [mm ³]	Dielectric Material	Feeding System	RL [dB]	Radiation Pattern	Gain in dBi	Power Losses
[35]	10.94	28×28×8.4	FR4	50Ω strip line	~ 25	Multi-Lobes	8.17	High
[36]	9.6	27.5×42.5×1.57	FR4	50Ω strip line	~ 40	Multi-Lobes	~4.0	High
[37]	9.7	50×30×1.6	FR4	50Ω strip line	~ 25	Multi-Lobes	2.09	High
[38]	8.2	40×40×3.2	FR4	50Ω strip line	~ 28	Bidirectional	7.023	High
[39]	8.94	50×30×1.6	FR4	50Ω strip line	~ 30	Bidirectional	~5.5	High
[40]	10	46.7×46.7×3.2	FR4	4 Apertures	~ 30	Bidirectional	2.5 dBic	Very High
[41]	10	13.39×9.16×4.4	Rogers RO3003	50Ω CPW line	26	Bidirectional	6.72	High
[42]	8.95	34×36×1.6	FR4	50Ω strip line	15	Bidirectional	2.63	Very High
[43]	11	32×32×1.6	FR4	50Ω strip line	~ 15	Bidirectional	2.2	High
[44]	9	25×26×1.6	FR4	50Ω strip line	~ 25	Bidirectional	6.2	High
[45]	8.15	37×35×3.4	Laminate	Aperture	~ 22	Bidirectional	5.33	High
[46]	8.19	80×36×1.575	RT-Duroid 5880	50Ω SIW line	~ 25	unidirectional	9.6	Medium
[47]	9	20×20×2.5	FR4	50Ω coaxial probe	low	unidirectional	Not assigned	high
[48]	10.5	22.5×22.5×2	Mg-Nd-Cd ferrite	50Ω coaxial probe	~ 30	unidirectional	0.46	Low
Cross-patch antenna	8.40	32.4×48.9×1.5	Rogers 5880	50Ω strip line	26.5	unidirectional	8.3	Minimum
Metasurfaced antenna	8.40	32.4×48.9×3	Rogers 5880	50Ω strip line	31.31	unidirectional	~10.0	Minimum

The operating frequencies of all studied designs are in the X-band, and the majority of investigated designs radiate unidirectionally, resulting in negligible interference with other CubeSat components. As a result, any increased value in antenna gain, beamwidth angle, and impedance bandwidth, or size reduction is beneficial for CubeSat applications. All of this is related to the CubeSat box's restricted physical dimensions, limited power for exciting numerous electronic equipment, limited daily communication length with the CubeSat, and the short lifespan of most deployed AeroCube projects. This implies that the lack of any human CubeSat interaction after the CubeSat is launched into orbit makes any upgrade of the overall mission parameters incredibly efficient for consumers and engineers who are operating earth stations on Earth. Hence, both of the cross-patch antenna with and without metasurface have the smallest dimensions, operate over a broader impedance bandwidth, have the maximum antenna gain, and have a wider 3 dBi gain bandwidth when compared to the metasurfaced antenna designs de-tailed in [25]. In comparison to the metasurfaced antenna design provided in [29], it is bidirectional, resulting in substantial interferences with other components within the CubeSat body due to increased temperature and hence resistance to electrical circuits. This design, therefore, cannot be utilized for CubeSat applications without a metallic reflector beneath its back face or the use of a deployment device to launch this antenna system after the CubeSat launch to make the antenna attached axially to the CubeSat's corner. As a result, this antenna design is not a suitable fit for CubeSats since it increases the chance of mission failure whether used in its current form or in conjunction with a deployment mechanism to launch the antenna after the CubeSat is in its target orbit. Compared to all other metasurface antenna approaches presented in Tables 3 and 4, our configured cross-patch antenna alone and the optimized metasurface antenna design allow for greater gain, the smallest space, the usage of very little electric energy, and a very low-cost CubeSat antenna system. As a consequence, the created antenna approaches yield the best performances that satisfy all CubeSat requirements. Furthermore, the results shown in Table 5 compare the generated antenna designs to certain patch antenna systems produced by the scientific community for X-band applications.

Geometrically, antenna configurations proposed in [35-37] satisfy all geometrical and mechanical criteria of all CubeSat configurations while their radiation pattern are multi-lobes and hence their major weakness that limits their effectiveness for space uses is the very high interferences with other circuits inside the satellite box. From another hands, they give gains below 10 dBi and so the metasurface antenna developed in this study measures the superior gain with advantages of lowest volume and low cost at X-band. Contributions detailed in [38-45] describe antenna systems meet all geometrical and mechanical criteria for all CubeSat standards while their very high back lobe radiations limit their suitability for operation on CubeSats. They present very high losses and

allow to very high interferences that increase the failure rate. Despite its unidirectional radiation pattern, small dimensions and good stiffness, the antenna design developed by authors of [47] is unsuitable for integration with CubeSats due to its very low return loss and low gain at X-band. Likewise, it presents huge losses of electrical energy that is very constrained on CubeSats. The approach presented in [48] leads to obtain very low gain at X-band (0.46 dBi) that can be used only for some nearfield applications under certain circumstances. Thus, it doesn't gratify the appropriateness criteria of CubeSat missions. Compared with antenna systems developed in [46], our configured metasurface antenna allows obtaining the superior gains, holding the lowest volume, using up very low electric energy and is very low cost CubeSat antenna system. As a result, our metasurface antenna system leads to obtain the highest performances that meet all CubeSat criteria among all cited antenna approaches.

5. CONCLUSIONS AND PERSPECTIVES

This research project develops a tiny size cross-patch antenna design with and without a metasurface based on experimental measurements for smallest unlimited lifetime CubeSats. Both the metasurfaced antenna and the cross-patch antenna by itself are lightweight, low power consumption, and have mechanical and geometrical characteristics that make them very suitable with all CubeSat designs, including 0.5U and 1U forms. Simulations and experimental measurements that show high agreement prove that both the cross-patch antenna and the metasurfaced antenna radiate unidirectionally and function over large impedance bandwidths in the X band. Furthermore, despite its small size, the metasurface antenna measures a peak gain of around 10.0 dBi, demonstrating a gain improvement of roughly 2.0 dBi and 3 dBi gain bandwidths greater than 1.0 GHz, whereas the cross-patch antenna alone produces a peak gain of more than 8.0 dBi. In addition to that, both antenna configurations exhibit broad HPBW at 8.4 GHz and substantial return losses (RLs), indicating excellent performance for advanced low-earth orbit CubeSat missions.

As a starting point for future research, we may construct a multilayer Fabry-Perot antenna using the same metasurface or new arrays of unit cells to boost the antenna gain to over 20 dBi, making it suitable for 1U CubeSats at the same CubeSat frequency. This would further reduce the amount of antenna gain required for the deployed earth station to maintain connections with the CubeSat in its orbit while traveling around the planet at high speeds multiple times each day.

ACKNOWLEDGMENT

The authors express their appreciation to the ECE department at LKCTC and O.Ya.Usikov Institute for Radiophysics and Electronics of NAS of Ukraine for their significant help and encouragement throughout this research.

REFERENCES

1. C. Cappelletti, D. Robson, *CubeSat Missions and Applications*, 53 (Cubesat Handbook, Academic Press: 2021).
2. J. Vanreusel, *Launching a CubeSat: Rules, Laws, and Best Practice*, 391 (Cubesat Handbook, Academic Press: 2021).
3. L.K. Slongo, S.V. Martínez, S.B.V.B. Eiterer, E.A. Bezerra, *Int. J. Circ. Theor. Appl.* **48**, 2153 (2020).
4. S.A. Khan, Y. Shiyu, A. Ali, S. Rao, S. Fahad, W. Jing, J. Tong, M. Tahir, *Adv. Space Res.* **69** No 10, 3741 (2022).
5. A. Al Mahmood, P.R. Marpu, *IEEE J. Miniatur. Air Space Syst.* **5** No 2, 85 (2024).
6. Y.-Y. He, S.-H. Tsai, H.V. Poor, *IEEE Trans. Sign. Proc.* **72**, 2783 (2024).
7. A. Kazemnia, A. Dutt, L. Wang, A. Garg, E. Resnick, G. Bussey, *IEEE Aerosp. Conf.*, 1 (2024).
8. J. Jiao, P. Yang, Z. Du, Y. Wang, R. Lu, Q. Zhang, *IEEE Trans. Vehicular Techn.* **73** No 9, 1 (2024).
9. Y.S. Bondarenko, D.A. Marshalov, B.M. Zinkovsky, A.G. Mikhailov, *Astr. Lett.* **50** No 1, 92 (2024).
10. D. Nakayama, K. Sano, T. Matsushima, Y. Fukumoto, *Intern. Conf. Electr. Pack.* 193 (2024).
11. S. Saha K. Dasala, *49th Intern. Conf. Infrared, Millim., THz Waves (IRMMW-THz)*, 1 (2024).
12. E.S. Hope, D.W. McKenney, L.M. Johnston, J.M. Johnston, *PLoS 1*, **19** No 5, e0302699 (2024).
13. M. Crews, L. Grootboom, *IEEE Radar Conf. (RadarConf24)*, 1 (2024).
14. N. Supreeratitukul, P. Akkaraekthalin, S. Kawdungta, C. Phongcharoenpanich, *12th Intern. Electr. Eng. Congress (IEECON)*, 1 (2024).
15. M.M. Migalin, V.G. Koshkid'ko, V.V. Demshevsky, *Radiation and Scattering of Electromagnetic Waves (RSEMW)*, 188 (2023).
16. D. Subitha, S. Velmurugan, M.V. Lakshmi, P. Poonkuzhali, T. Yuvaraja, S. Alemayehu, *Adv. Mater. Sci. Eng.* 4319549, 1 (2022).
17. I. Surjati, S. Alam, L. Sari, Y.K. Ningsih, A. Elishabet, S.M. Putri, Z. Zakaria, T. Firmansyah, *J. Nano- Electron. Phys.* **16** No^o2, 02009 (2024).
18. G.H. Mebarki, N. Benmostefa, *J. Nano- Electron. Phys.* **16** No^o1, 01002 (2024).
19. B.T.P. Madhav, J. Vani, R.R. Priyanka, B.P. Nadh, M.C. Rao, *J. Phys.: Conf. Ser.* **1804** No 1, 012191 (2021).
20. O. Borazjani, M. Naser-Moghadasi, J. Rashed-Mohassel, R.A. Sadeghzadeh, *Int. J. Microwave Wireless Technol.* **12** No 9, 906 (2020).
21. R. Rajkumar, K.U. Kiran, *In Optical and Microwave Technologies: Select Proceedings of ICNETS2 IV*, 91 (2018).
22. M. Gaharwar, D.C. Dhukarya, *IETE J. Res.* **69** No 4, 2015 (2023).
23. J. Jiang, Y. Li, L. Zhao, X. Liu, *The Applied Computational Electromagnetics Society Journal (ACES)*, 556 (2020).
24. A. Majeed, J. Zhang, H.A. Khan, *Research Square* (2024).
25. S. Charola, S.K. Patel, J. Parmar, R. Jadeja, *J. Electromagn. Waves Appl.* **36** No 2, 180 (2022).
26. D. Samantaray, S. Bhattacharyya, *IEEE Trans. Anten. Propag.* **68** No 9, 6548 (2020).
27. R. Swain, D.K. Naik, A.K. Panda, *IET Microwaves, Anten. Propag.* **14** No 11, 1216 (2020).
28. M. Guo, W. Wang, P. Huang, *IET Microwaves, Anten. Propag.* **14** No 9, 919 (2020).
29. S. Genovesi, F.A. Dicandia, *IEEE Access* **10**, 88932 (2022).
30. J. Wang, W. Wang, A. Liu, M. Guo, Z. Wei, *IEEE Anten. Wireless Propag. Lett.* **20** No 3, 337 (2021).
31. L. Leszkowska, M. Rzymowski, K. Nyka, L. Kulas, *IEEE Anten. Wireless Propag. Lett.* **20** No 11, 2090 (2021).
32. S. Dey, S. Dey, *IEEE Access* **12**, 65981 (2024).
33. B. Feng, J. Lai, Q. Zeng, K.L. Chung, *IEEE Access* **6**, 33387 (2018).
34. B. Benhmimou, N. Hussain, N. Gupta, R.A. Laamara, S.K. Arora, J.M. Guerrero, M. El Bakkali, *Data Analytics for Internet of Things Infrastructure* **2023**, 117 (2023).
35. D. Samantaray, S. Bhattacharyya, *IEEE Trans. Anten. Propag.* **68** No 9, 6548 (2020).
36. N. Kaur, A. Kaur, *Wireless Pers. Commun.* **109**, 1673 (2019).
37. K. Mahendran, R. Gayathiri, H. Sudarsan, *Microprocessors and Microsystems* **80**, 103400 (2021).
38. R. Anand, P. Chawla, *Int. J. RF Microw. Comput. Aid. Eng.* **30**, e22277 (2020).
39. B. Bag, P. Biswas, S. De, et al, *Wireless Pers. Commun.* **111**, 411 (2020).
40. A. Bhattacharya, B. Dasgupta, R. Jyoti, *Int. J. RF Microw. Comput. Aid. Eng.* **31**, e22505 (2021).
41. Y. Han, S. Gong, J. Wang, Y. Li, S. Qu, J. Zhang, *IEEE Trans. Anten. Propag.* **68** No 3, 1419 (2020).
42. A. Eslami, J. Nourinia, C. Ghobadi, M. Shokri, *Int. J. Microwave Wireless Technol.* **13** No 8, 859 (2021).
43. B. Mishra, *Microw. Opt. Technol. Lett.* **61**, 1857 (2019).
44. K. Srivastava, B. Mishra, A.K. Patel, R. Singh, *Microw. Opt. Technol. Lett.* **62**, 3301 (2020).
45. T. Tewary, S. Maity, S. Mukherjee, A. Roy, P.P. Sarkar, S. Bhunia, *AEU – Int. J. Electron. Commun.* **139**, 153905 (2021).
46. M.V. Yadav, S. Baudha, S.C. Singam, *7th Uttar Pradesh Section International Conference on Electrical, Electronics and Computer Engineering (UPCON)*, 1 (2020).
47. G.P. Mishra, B.B. Mangaraj, *IET Microw. Anten. Propag.* **13**, 1593 (2019).
48. S.R. Bhongale, *J. Magn. Magn. Mater.* **499**, 165918 (2020).

Проектування, виготовлення та вимірювання X-смужової антени типу «cross-patch» з метаповерхнею для перспективних місій CubeSat на орбітах LEO

Б. Бенхмімоу¹, Ф. Омари¹, Н. Гупта², К. Ель Хадірі³, А. Когут⁴, Р.А. Лаамара¹, І. Кузьмичев⁴,
М. Ель Баккалі^{1,3}

¹ LPHE-MS, факультет наук, Університет Мухаммеда V у Рабаті (UM5), Рабат, Марокко

² Кафедра електроніки та зв'язку, Технічний кампус коледжу Лаялтур Кхалса, Джаландхар, Пенджаб, Індія

³ Кафедра фізики, факультет наук Ель Джадіда, Університет Шуайб Дукаслі, Ель Джадіда, Марокко

⁴ Інститут радіофізики та електроніки ім. О.Я. Усикова НАН України, 61085 Харків, Україна

У даному дослідженні було розроблено, мініатюризовано та оптимізовано розумну антену з метаповерхнею, яка відповідає вимогам найменших одиниць CubeSat з мінімальним аеродинамічним опором на заданій висоті. Однією з основних цілей є продовження часу експлуатації супутників AeroCube, використовуючи вищі орбіти та забезпечуючи значні кути НРВW (ширина променя на півпотужності), щоб збільшити період прийому даних протягом доби при ефективному енергоспоживанні. Для досягнення цього було застосовано нову форму антени — планарні дипольні елементи, розташовані перпендикулярно один до одного, що дозволяє максимально зменшити розміри без погіршення робочих характеристик. При цьому конструкція не потребує жодних розгортальних механізмів після виходу супутника на орбіту. Також було впроваджено та оптимізовано нову форму елементарної комірки метаповерхні, що дало змогу додатково покращити характеристики кінцевої антени в X-смужі та, відповідно, ефективність усього CubeSat. Виготовлена антена з метаповерхнею була успішно протестована в безеховій камері та за допомогою векторного аналізатора мережі, продемонструвавши задовільні результати в X-смужі для комунікаційних систем CubeSat: легка конструкція, спрямована діаграма випромінювання, широка смуга пропускання при підсиленні 3 дБ (близько 1,0 ГГц), високе підсилення $\approx 10,0$ дБі при 8,4 ГГц. Загальні результати щодо габаритів і об'єму є оптимальними для CubeSat місій з тривалим терміном служби в X-смужі для будь-яких конфігурацій CubeSat (1U і більше).

Ключові слова: 1U CubeSat, Вимірювання антен, Cross-patch антена, Тривалість місії CubeSat, МТМ (метаматеріали), Пікове підсилення.